Integration of Edge-Lit Quantum Dot Coated Lightguides in Soft Smart Surfaces

Ravi Kishore, Jan Audenaert, Frederick Bossuyt, Pieter Bauwens, Bjorn Vandecasteele, and Youri Meuret

***Abstract*—Soft smart surfaces, integrating flexible electronics and decorative materials, seamlessly combine sensors and light-emitting elements for user interaction. This allows minimalist designs for automotive interiors. To integrate uniform light-emitting elements into flexible materials, printed emissive layers like OLEDs or QLEDs can be used. These offer saturated colors but face challenges in cost, brightness, efficiency, and durability. Backlight-based technologies, such as edge-lit planar lightguides, provide a mature alternative. However, embedding such lightguides into thin, flexible stacks poses significant challenges, particularly in maintaining total internal reflection due to the need for air gaps. This work presents the design and fabrication of an edge-lit lightguide with a quantum dot (QD) color conversion layer, fully integrated into a soft, flexible polyurethane resin (PUR) layer laminated on a polyethylene terephthalate (PET) substrate containing electronic circuitry and blue LEDs. The spreading of the light within the lightguide, to obtain uniform light-emitting icons and symbols, is realized by employing diffuse reflective paint layers and optimizing the lightguide shape. Optical ray tracing simulations, based on accurately measured material properties, were used to determine the required QD loading in the 100 μm thick QD layer to achieve the targeted color, as well as analyze the performance of the configuration in detail. The final design was validated through light output measurements from a fabricated prototype.**

***Index Terms*—Edge-lit lightguides, flexible lightguides, optical modeling, quantum dot color conversion, ray tracing, soft smart surfaces.**

I. Introduction

A CLEAR trend in the automotive industry is the increased integration of advanced technology into the interior and exterior surfaces of vehicles, while maintaining a minimalist and unobtrusive appearance. A growing number of electronic components and devices are incorporated into the vehicle surfaces to support human-vehicle interaction [1]. Apart from sensors to detect human action, light-emitting devices for visual feedback are crucial. In the past, there was a clear separation between interior surfaces with a decorative purpose (often soft surfaces) and surfaces for user input and information output (typically hard surfaces). This boundary has recently blurred with the advent of soft, interactive/smart surfaces that provide a seamless integration of both control and display elements. Such soft smart surfaces are fabricated with stretchable and flexible decorative materials (e.g. polyurethane or polyvinyl chloride), laminated on flexible electronic substrates with all the required electronic and optical components. Examples are the "shy tech" concept introduced by BMW [2], [3], and the smart surface technology of Yangfeng Automotive Interiors [4], [5]. Soft smart surfaces are a subclass of flexible electronics: a field undergoing much research and development as it has far reaching applications in many other fields such as aviation, wearable electronics and biomedicine [6], [7].

To integrate light-emitting elements into soft and flexible materials there are several possible approaches. The most straightforward manner is the integration of one or more light emitting diodes (LEDs) in a particular configuration, e.g. as a single point source, a line of point sources or a 2D matrix. Compact LED packages can be mounted on the flexible electronic substrate via existing soldering and reflow soldering processes, or via flip-chip bonding. Creating uniformly emitting areas is however challenging when working with individual LEDs. An alternative is therefore to print thin, flexible light emissive layers on the electronic substrate. Possible technologies include alternating current powder electroluminescent devices (ACPELs), light emitting electrochemical cells (LECs), and organic light emitting diodes (OLEDs) [8]. OLEDs are seeing the most rapid development among these flexible self-emissive technologies. They rely on emitting polymer layers sandwiched between flexible transport layers attached to flexible electrodes [9]. Quantum dot light-emitting diodes (QLEDs) is another highly researched self-emissive technology where the emitting layer is made up of quantum dots (QDs) [10]. Quantum dots are semiconductor particles of size 1 to 10 nm that exhibit sharp luminescence peaks at high photoluminescent quantum yield (PLQY). Engineering the QD size and size distribution allows tailoring of the emission wavelength peak and spectral width, respectively [11], which in turn makes possible the fabrication of display devices with wide color gamut and saturated colors [12].

Despite the promise of OLEDs and QLEDs for fabricating flexible light-emitting elements and displays, there are still significant challenges in terms of lifetime, efficiency, brightness, and cost [13], [14], [15]. This explains why most displays today are still backlight based, i.e. an LCD panel homogeneously illuminated by a separate backlight. This backlight consists

Received 3 July 2025; accepted 6 August 2025. Date of publication 11 August 2025; date of current version 20 August 2025. This work was supported in part by Flemish government, VLAIO (Flanders Innovation & Entrepreneurship) under Contract HBC.2020.2377 and Contract HBC.2022.0682. *(Corresponding author: Ravi Kishore.)*

Ravi Kishore, Jan Audenaert, and Youri Meuret are with the Department of Electrical Engineering (ESAT), Light & Lighting Laboratory, KU Leuven, 9000 Ghent, Belgium (e-mail: ravi.kishore@kuleuven.be).

Frederick Bossuyt, Pieter Bauwens, and Bjorn Vandecasteele are with the Centre for Microsystems Technology (CMST), IMEC and Ghent University, 9050 Zwijnaarde-Gent, Belgium.

Digital Object Identifier 10.1109/JPHOT.2025.3597397

typically of a planar lightguide with outcoupling structures, illuminated from the side by an array of white LEDs. Backlight based displays are still superior to self-emissive displays in terms of brightness, resolution, lifetime and cost, while the latter offer superior response time, color gamut, black state and an ultra thin profile [15]. The saturated colors that can be achieved with OLEDs and QLEDs can also be realized with a backlight, by adding a QD foil on top of the lightguide that is then illuminated with blue LEDs. The light of the blue LEDs is then partially converted into saturated green and red colors, when the extracted light from the lightguide passes the QD foil [16].

Considering the maturity of backlight based technology, it has also been considered for developing flexible displays. So far, demonstrations of backlight based flexible displays are few as they require printing a high-viscosity liquid crystal monomer solution between flexible plastic substrates, and a flexible backlight film that is illuminated by an array of LEDs [17]. In the work of Chen et al. [18], a thin curved lightguide of thickness 1.4 mm is employed on which an array of QD structures is screen printed, each containing a mixture of red/green QDs and light scattering particles. The limited thickness of the lightguide allows the fabrication of a curved display, but it does not achieve full flexibility in the strict sense.

The use of a flexible planar lightguide with QDs, edge-lit by blue LEDs, is thus a potential approach to integrate uniform light-emitting elements with saturated colors and high output luminance, in soft smart surfaces for automotive applications and beyond. However, edge-lit lightguides operate on the principle of Total Internal Reflection (TIR) at the top and bottom interfaces of the lightguide, to spread the incoming light over the complete lightguide area. Creating air gaps above and below a lightguide that is embedded within a thin, flexible stack consisting of a decorative material layer and electronic substrate, is however very challenging.

In this work we present the optical design and fabrication of an edge-lit backlight configuration with a QD color conversion layer that is fully integrated in a soft flexible Polyurethane Resin (PUR) layer, laminated on a polyethylene terephthalate (PET) layer. This PET layer carries all the electronic circuitry and components, including the blue LEDs that inject light in the lightguide layer at its edges. The issue that air gaps cannot be used to induce TIR, is solved by using diffuse reflective paint layers on top of the lightguide and modifying the shape of the lightguide to ensure uniform illumination of certain icons and symbols. Realizing sufficient color conversion in the QD layer is quite challenging as the thickness of the QD layer is limited to 100 μm. To achieve this, a good estimate of the required QD loading is required and a suitable resin has to be identified to support the high QD concentration.

Optical ray tracing simulations in Light Tools [19] were used to design a prototype. Optical properties of all the materials comprising the full flexible stack were measured and fed to the model. The design was optimized for high output luminance, uniformity and the desired output color. Finally, the model was validated by measurements of the light output from a manufactured prototype.

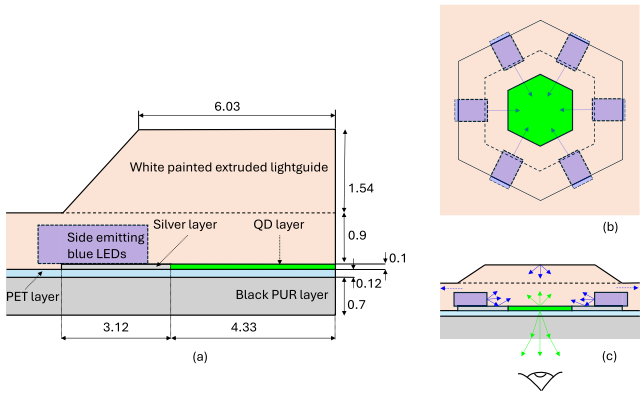

Fig. 1. (a) Exploded side view where layer thicknesses (in mm) are drawn to scale. (b) Top view. (c) Side view of the optical configuration with the viewing direction.

II. Optical Modeling

A. Optical Configuration

The layers comprising the flexible stack for illuminating a hexagonal icon (as an example) are shown in Fig. 1. The bottom layer is the side from which the icon is to be viewed. The flexible electronic substrate is a 0.12 mm thick PET layer onto which the required electronic circuitry is printed and the electronic components are mounted. Six side-emitting blue LEDs are positioned at the borders of a hexagonal reflective silver layer that is also printed on the PET layer. At the center of this hexagonal reflective surface, there is a hexagonal aperture through which the light can pass. A 0.9 mm thick flexible transparent lightguide, made from PUR, is deposited via cold spray additive technique on top of the hexagonal silver layer in the shape of a truncated hexagonal pyramid with a hexagonal base. The six side-emitting blue LEDs inject their emitted light in this hexagonal base. PUR is typically not a transparent material and has to be chemically modified to increase its transparency and enable its use as a flexible lightguide material. The full lightguide structure is covered with a white, reflective, diffuse paint layer, that prevents the injected light from escaping the structure, except via the hexagonal aperture in the silver layer. The multiple reflections at this paint layer and the silver layer homogenize the light that passes the hexagonal aperture. The exact shape of the truncated hexagonal pyramid is optimized to maximize the efficiency and uniformity of the emitted light distribution. Other light-emitting icons and symbols can be easily made by replacing the hexagonal aperture with another shape. On the other (bottom) side of the PET layer, the decorative layer is deposited, which is a 0.7 mm thick black PUR layer. While this translucent, partially absorbing layer, significantly reduces the efficiency of the light emission from the full stack, it is required to visually shield the underlying electronics (especially when there is no light emission), and realize the desired black matte appearance of the soft smart surface. To balance appearance with optical efficiency, several PUR formulations with varying black pigment concentrations (Fig. 8(a)) were tested. The formulation with pigment concentration of 0.5 cp (parts per 100 of base resin) offering the highest transmittance (8.6% for a 0.7 mm thick

layer at a wavelength of 530 nm) while maintaining sufficient concealment was selected to prepare the optical design.

In order to create light-emitting elements with a different color than the light of the used blue LEDs, a 100 μm thick layer of quantum dots mixed in a suitable resin, is deposited above the aperture, before depositing the lightguide layer on the PET substrate. This QD layer acts as a color converter layer and converts the blue light into another (saturated) color, before it escapes from the lightguide through the shaped aperture. The advantage of using QDs over working with additional green/red LEDs, is that it allows to use the same blue LEDs for all light-emitting elements that are integrated in the soft smart surface, independent of the emitted color. Blue LEDs are also known to have the highest external quantum efficiency (much higher than of green- and yellow-emitting LEDs) [20] and have superior thermal stability [21].

Fig. 1 also illustrates that the lightguide, PET and black PUR layers are continuous layers that are shared across multiple light-emitting icons, while the silver and QD layers are confined to individual icons. Light leakage via the lightguide layer can lead to optical crosstalk between adjacent icons. This can be prevented by limiting the thickness of the light guide layer outside the truncated pyramid area. However, manufacturing constraints can impose a lower limit to this light guide thickness.

B. Simulation Model

The configuration described in Section II-A was implemented in the optical ray-tracing software LightTools, utilizing accurately measured properties for all materials and interfaces. To model the color conversion functionality of the QDs, three key parameters are required: (i) the wavelength dependent absorption coefficient, (ii) the emission spectrum and (iii) the PLQY of the QDs [22]. The absorption coefficient represents the inverse of the mean free path, which defines the average distance a photon travels within the QD layer before being absorbed by a QD particle. The PLQY indicates the probability that an absorbed photon is down-converted into another photon, while the emission spectrum characterizes the probability distribution of these converted photons across different wavelengths. To create the color conversion layer, the QD dispersion is mixed with a UV-A curable 'thiol-ene' resin [23]. However, in order to accurately measure the QD modeling parameters, a highly dilute QD solution (10 μl of the original QD dispersion in 1000 μl toluene) is used to minimize the impact of QD re-absorption events [22].

The transmittance (T) of a collimated beam of light with path length $(x = 10$ mm) through this QD solution in a cuvette is measured with a Perkin Elmer 'Lambda 650S' spectrophotometer. The absorption coefficient (μ) is then derived following Beer-Lambert's law:

$$T(\lambda) = e^{-\mu(\lambda)x} \quad \Leftrightarrow \quad \mu(\lambda) = -\frac{\ln[T(\lambda)]}{x} \tag{1}$$

The resulting absorption coefficient corresponds to the concentration of QDs within the measured solution. To model the effect of varying QD concentrations in the layer, it suffices to scale this absorption coefficient by the appropriate scaling factor. To account for the absorption by the resin in which the QDs are mixed, this quantity is also measured and incorporated into the model, although it is quite low (0.005 mm^{-1} at 450 nm).

The emission spectrum and PLQY of the QDs was measured using an Oriel Instruments '74055 MS260i' spectrometer linked to a GigaHertz Optik 'ODM98' coated integrating sphere [24], utilizing the same highly dilute QD solution. The PLQY of the QDs was measured to be 75 %. The measured values for the emission and absorption spectrum are shown in Fig. 2(a). The overlap between these two spectra indicates that some amount of color converted light undergoes re-absorption; an effect that is known to have a significant impact on the color conversion efficiency. The normalized spectral radiant flux of the used side-emitting SMD LEDs (LTST- 020TBKT from LITE-ON Technology Corp) is also shown in Fig. 2(a). The LED chip emitting area is 1.7×0.7 mm and its typical emission peak is at 470 nm.

The model also includes the measured reflectance values (diffuse and specular) of the lightguide and PET coating (see Fig. 2(c)). The absorption coefficient for the light guide material and black PUR material are derived from transmittance measurements on layers with known thickness, following (1). The reflectance and transmittance values were measured with an 'Ultrascan Pro' spectrophotometer (Hunter Labs). The black PUR layer is highly pigmented, resulting in substantial absorption. From the absorption values shown in Fig. 2(b) it is clear that a major factor limiting the output flux is the black PUR layer after the aperture.

C. Simulation Methodology

The optical simulations were used to analyze the impact of the QD concentration and QD layer thickness on the resulting color point and output power. For increasing values of the QD absorption coefficient, the average chromaticity (x,y) value at the output aperture was simulated till it reaches close to the target Adobe RGB color space green primary chromaticity [25] as can be seen in Fig. 3(a). This process is repeated for three different layer thicknesses: 25, 50 and 100 μm. The blue and green component of the output flux versus the QD absorption coefficient (@450 nm) are plotted in Fig. 3(b). For a given thickness, the blue component is increasingly absorbed and converted to the green component, as the QD concentration increases. The decrease of the blue component is almost exponential according to Beer-Lambert's law, while the green component first increases as more blue light is converted but then slowly decreases due to increased re-absorption losses at higher QD loading. Note that the peak of the green flux does not coincide with the optimal absorption coefficient for reaching the targeted green primary.

To reach this green primary with a 100 μm QD layer, the required volumetric concentration of QDs in the resin is 800 times higher than the QD concentration of the solution used for measuring the absorption coefficient. For the 50 and 25 μm QD layers, the QD concentration should, to a good approximation, be proportionally higher as 1/thickness, as can be verified in Fig. 3(b). The simulation results also demonstrate that the green

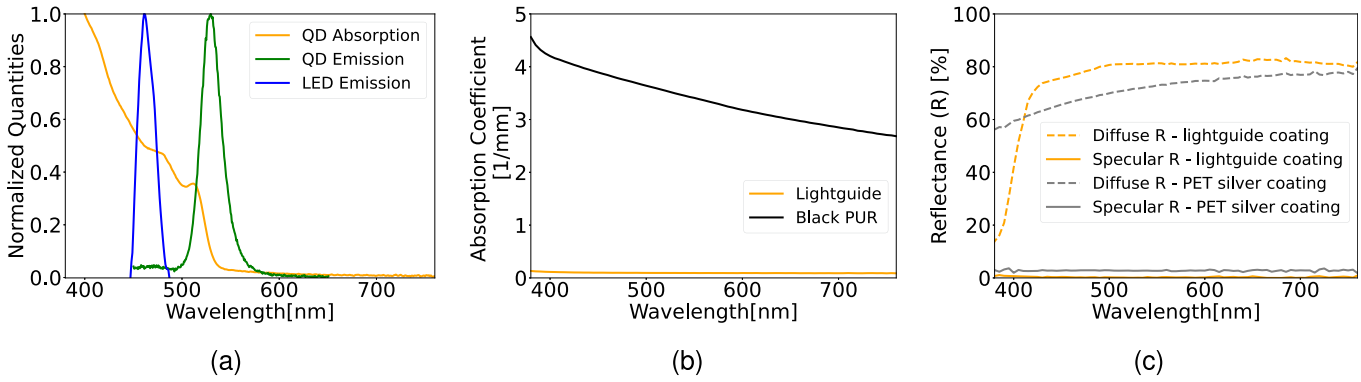

Fig. 2. (a) Measured absorption and emission of green emitting QDs, and normalized spectral radiant flux of the side emitting LEDs. (b) Measured absorption and (c) reflectance for various layers comprising the flexible stack.

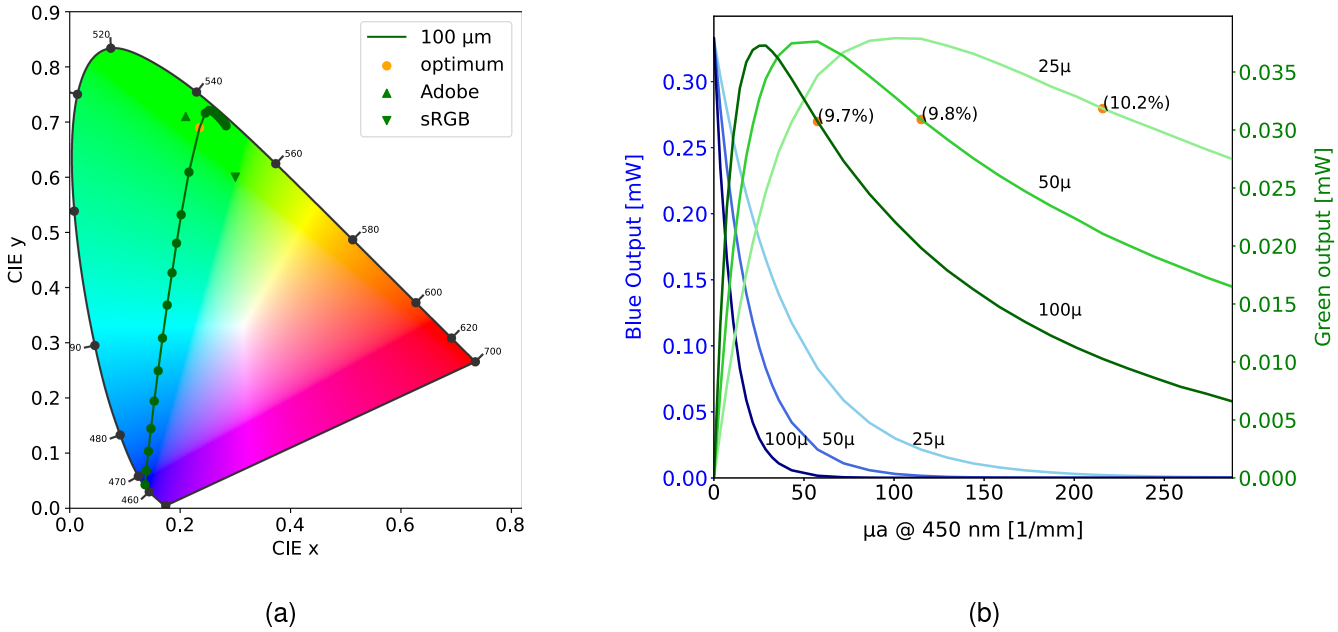

Fig. 3. Graphs depicting the used simulation methodology to choose the optimal QD concentration and layer thickness. (a) The locus of the average output chromaticity (in CIE 1931 color space for a standard observer) with varying QD concentration for a 100 μm layer thickness. (b) Output flux as a function of the QD concentration for 3 different layer thicknesses. The blue and green lines denote the blue ($\lambda < 500$ nm) and green ($\lambda \geq 500$ nm) component of the output spectrum. The orange dots denote the point at which the desired chromaticity is best approached, while the % in brackets indicate the color conversion efficiency (2) at this point.

output flux, close to the targeted color point, is very similar for all layer thicknesses. Therefore, it was decided to proceed with a 100 μm layer since it allows for a lower QD concentration. A lower QD concentration supports easier curing of the layer since the amount of UV curable resin can be higher.

The optical simulations were also used to analyze the optical efficiency of the light-emitting element for different values of the QD absorption coefficient. Without QDs (i.e. $\mu = 0$), only blue light escapes from the hexagonal aperture and black PUR layer. The optical efficiency, defined as the ratio of the blue output flux to the total blue flux emitted by the 6 LEDs, is then equal to 0.4 %. When the QD loading is increased ($\mu > 0$) part of the blue light is converted into green light. The color conversion efficiency (η) of the light-emitting element is defined as the ratio of the green output flux to the blue output flux when no QDs are used:

$$\eta(\mu) = \frac{\Phi_{green,\,\mu}}{\Phi_{blue,\,\mu=0}} \tag{2}$$

This color conversion efficiency includes non-unity PLQY losses, Stokes losses (wavelength downconversion), reabsorption losses, and losses because half of the color converted light is emitted towards the injected lightguide which has poor recycling efficiency. The color conversion efficiency in case of the 100 μm layer with optimal QD loading for reaching the targeted color point is equal to 9.7 % (Fig. 3(b)). This results in a total optical efficiency of 0.04 %.

The total optical efficiency of this simulated system, which corresponds to the demonstrated system discussed in the next section, is clearly very low. An important reason for this limited

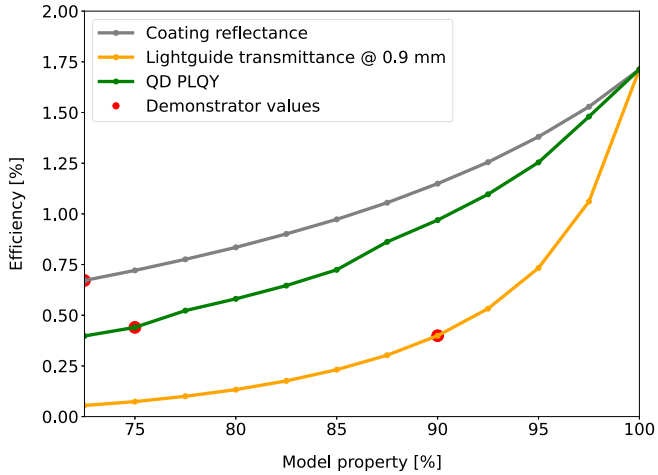

Fig. 4. Impact of the various material parameters on the simulated optical efficiency. When varying a parameter, the other parameters where chosen equal to 100 %. The red marks indicate the measured specifications for the materials used in the actual demonstrator.

efficiency is the low transmission through the black PUR layer, which is only 8.6 % (on-axis), and trapping of light in this layer due to TIR. However, as explained before, this black PUR layer is essential for the appearance of the soft smart surface. The other losses are induced by the light absorption in the light guide material, the reflection losses at the PET and light guide coating, the light leakage via the light guide layer, and the earlier mentioned color conversion losses.

To have an indication of the potential optical efficiency of the configuration, we start by considering the maximum achievable efficiency. This maximum efficiency is obtained with a fully transparent lightguide, coatings with 100 % reflectance, QDs with a PLQY of 100 %, and no lightguide leakage. Only Stokes losses and losses in the black PUR layer are considered, and still the simulated optical efficiency is only 1.71 %, illustrating the significant loss in the shielding layer.

In practice, the efficiency will be significantly lower due to material imperfections and fabrication constraints. To give an indication of the relative impact of the various material parameters on the system efficiency, optical simulations were performed using different values for the light guide transparency, QD PLQY, and coating reflectance, while leaving the other parameters ideal, and assuming no lightguide leakage (which is 7 % for a 0.9mm thick lightguide). These optical simulation results are presented in Fig. 4, where it can be seen that the lightguide transmittance has the greatest impact on efficiency, followed by the PLQY of the QDs, and the reflectance of the coatings.

III. Demonstrator Fabrication and Characterization

Green perovskite QDs (Q-520, procured from Avantama AG) available as a dispersion in toluene were mixed with 'Norland Optical Adhesive 88' (a transparent UV-A curable 'thiol-ene' polymer [23]) in a 8:1 volumetric ratio, as predicted by the simulations. UV curing of 100 μm thick QD layers was attempted using a 365 nm UV curing lamp with an irradiance

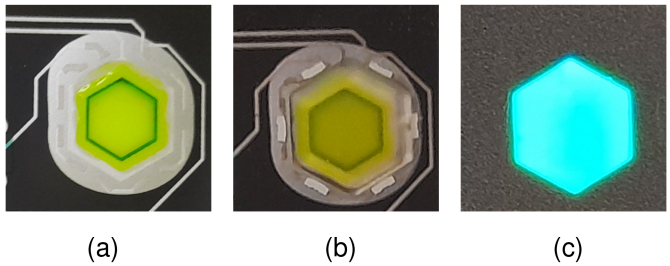

Fig. 5. (a) Screen printed QD layer on circuit printed PET substrate. (b) Side-emitting LEDs attached to the PET substrate, integrated with the PUR lightguide which is later painted white. (c) Final light-emitting element after affixing the black contrast layer to the reverse side of the PET substrate.

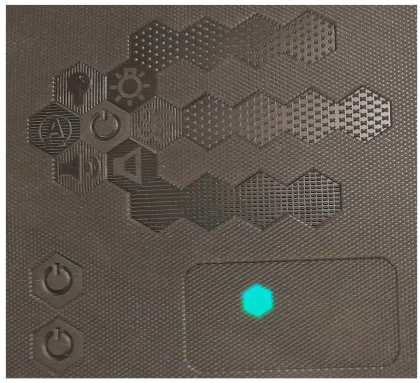

Fig. 6. Photograph demonstrating the visual shielding functionality of the black PUR layer, effectively concealing underlying electronics and enhancing surface appearance.

= 1.3 mW/cm^2 at the sample. It was found that these layers were difficult to cure as such, hence the QD-resin mixture was left for 15 hours in a fume hood to dry off the excess toluene. This 'dried' mixture was then stencil printed onto the PET layer containing the printed circuit as shown in Fig. 5(a), and UV curing was now successful. Blue LEDs coated with a suitable conductive adhesive were placed at the intended positions and the conductive adhesive was thermally cured at 150 °C. This process was followed by the deposition of the transparent PUR lightguide onto the PET layer using an additive spray coating technique, and the result is shown in Fig. 5(b). The top surface of the lightguide was further coated with a white paint layer functioning as a diffuse reflective coating. For the evaluation of the optical performance, a separate 0.7 mm thick black PUR layer was placed in optical contact with the PET layer on the opposite side of the printed circuit. Fig. 5(c) shows the light-emitting symbol when the LEDs are turned on. An illustration of the shielding functionality of the black PUR layer can be seen in Fig. 6.

The on-axis luminance distribution of the light emission was measured using a 'Technoteam LMK 98-4 color' luminance camera, before and after affixing the black shielding layer to the reverse side of the PET surface. These measured distributions are shown in Fig. 7(a) and (b), illustrating the significant drop in luminance when the black shielding layer is added. The measured distribution with shielding layer can be compared to the

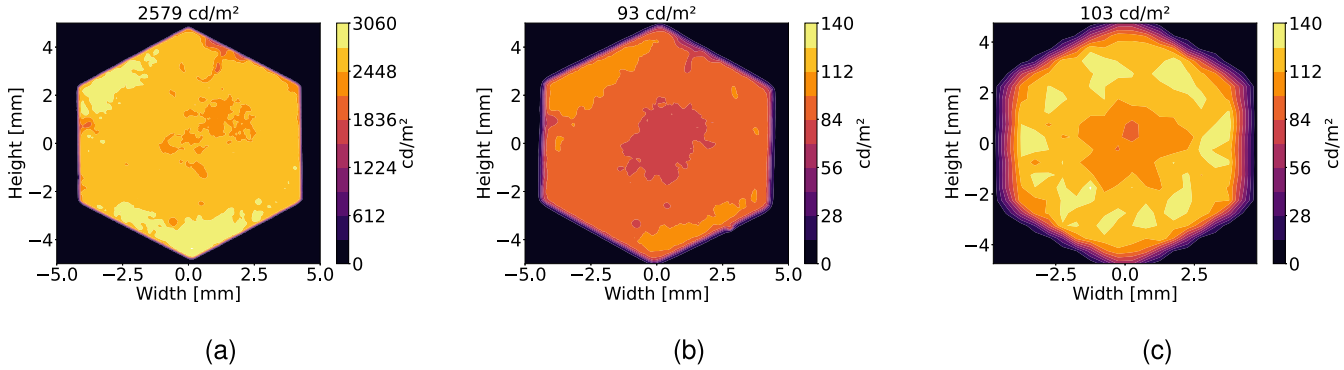

Fig. 7. Measured on-axis luminance distribution (a) without and (b) with the outer black layer of pigment concentration 1.0 cp (c) Simulated on-axis luminance distribution. The luminance values on top of each subfigure indicate the mean of the distribution.

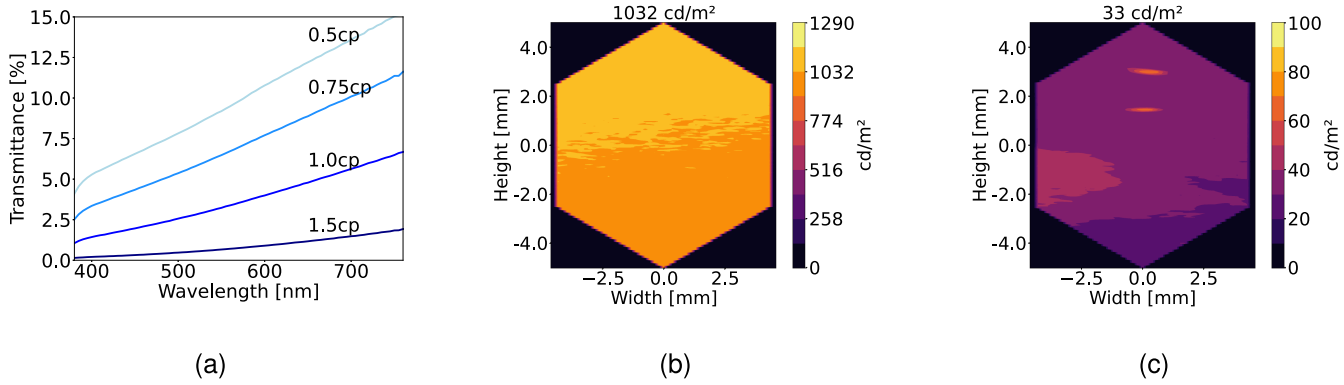

Fig. 8. (a) Measured transmittance of 0.7 mm thick black PUR layers containing various black pigment concentrations (cp refers to part per 100 part of base resin). (b) Measured on-axis luminance distribution of a commercial OLED module without and (c) with the black PUR layer (concentration of pigment 1.0 cp) placed on top in optical contact. The luminance values on top of subfigures (b) and (c) indicate the mean of the distribution.

simulated on-axis luminance distribution shown in Fig. 7(c). The average value of the measured luminance distribution (93 cd/m^2) is within 10 % of the average value of the simulated distribution (103 cd/m^2). It should be noted that the final demonstrator used a black PUR layer with a higher pigment concentration (1.0 cp) than the 0.5 cp assumed in the optical simulations. This difference in formulation accounts for the slightly lower measured luminance values compared to the simulated ones. The measured luminance uniformity (ratio of minimum to average) is larger than 80%, which is acceptable for this application. The light intensity distribution was also measured using a commercial near field Goniometer (Rigo 801-300, TechnoTeam GmbH) and the distribution was found to be lambertian, implying that the perceptual brightness of the icon remains the same irrespective of the viewing angle.

To position the above measured performance in the landscape of existing flexible technologies, a commercially available flexible white OLED module (Konica Minolta A88MA2B, peak luminance 1000 cd/m^2) was used as a reference emitter. This OLED was covered with black contrast layer carrying a pigment concentration of 1.0 cp (Fig. 8(a)). The measured on-axis luminance reduction observed for the OLED module is comparable to that for the QD-converted system when using the same black layer formulation (Fig. 8). This demonstrates that the optical losses introduced by the contrast layers are not unique to the QD implementation, but are a general challenge for any surface-emissive approach that requires to conceal internal structure while maintaining a soft, black, matte appearance.

The spectrum emitted by the light-emitting symbol was measured using a 'BWTEK Exemplar' spectrometer. Fig. 9(a) compares the measured spectrum with the simulated spectrum. One noticeable difference is the slightly higher blue region in the measured spectrum, potentially attributable to non uniformity in the layer. Additionally, a slight shift in the green emission peak is observed in the measured spectrum. This occurs because the emission spectrum of the QDs was modeled based on the measured emission spectrum at 450 nm excitation, while in practice, QDs absorb a range of wavelengths in both the blue and green region. Higher-wavelength excitation can cause slight red-shifts in the QD emission peaks [26].

The measured color coordinates across the full icon, shown in Fig. 9(b), were obtained using an 'LMK-98-4 Color Technoteam' camera. These measured results clearly reveal significant spatial color variations. The average measured variation in color coordinates $du'v'$ with respect to the target Adobe green primary was found to be 0.021. The simulated value of this color difference was only 0.012, and much less spatial color variation was present. An explanation for the differences

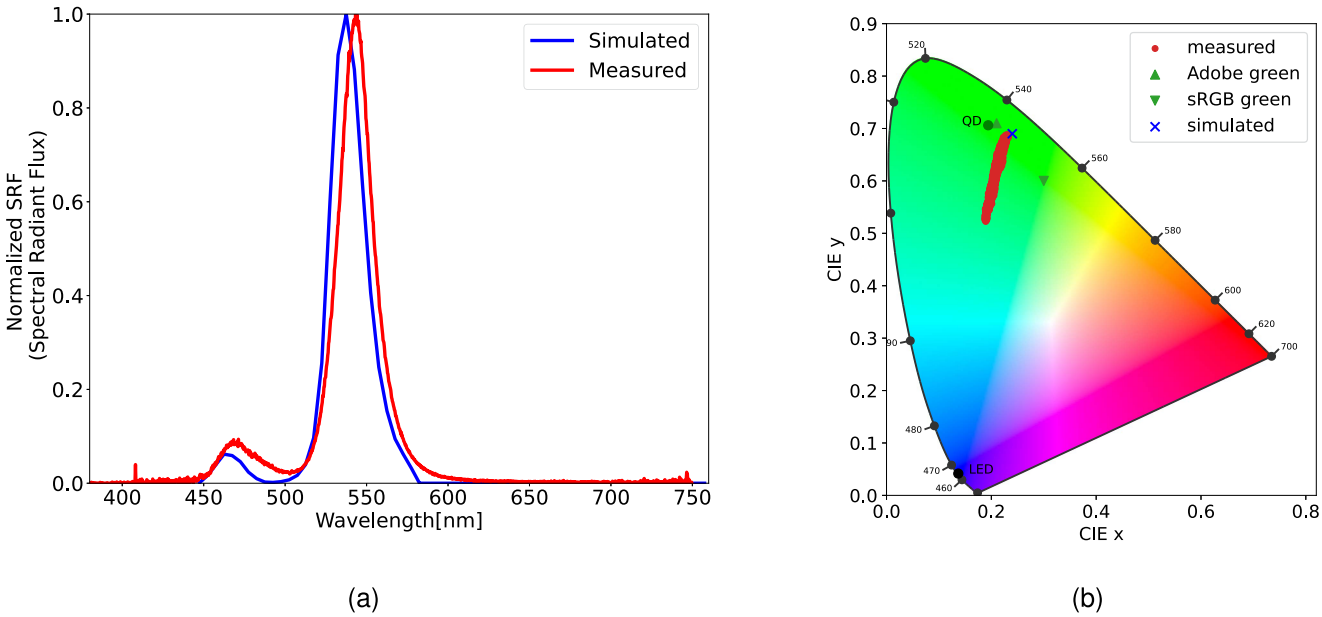

Fig. 9. (a) Comparison of measured and simulated spectrum. (b) Comparison of the measured chromaticity with chromaticity of the LEDs and QDs, simulated chromaticity of the device and that of the Adobe and sRGB standards.

between the experimental and simulated results are the slight thickness inconsistencies in the color conversion layer that can affect the resulting color point due to insufficient conversion in some places (as also inferred from the spectrum). Another factor is the inhomogeneous dispersion of QDs within the resin. This inhomogeneity likely results from the use of an off-the-shelf resin, which is not chemically tailored for optimal QD dispersion, leading to QD agglomeration. Such issues could be prevented by using a more dedicated binder for the QDs [27] and a more precise deposition method such as inkjet printing [28]. The QD layer was also exposed to elevated temperatures during curing of the conductive adhesive. This may have introduced irreversible reduction of photoluminescence intensity [29] which also leads to de-saturation in chromaticity. Nonetheless, while the measured color does not reach the highly saturated green primary chromaticity of Adobe RGB (0.21, 0.71), it is noticeably more saturated than the green primary in sRGB (0.3, 0.6).

IV. Conclusion

This study presented the design and fabrication of an edge-lit lightguide with a quantum dot (QD) color conversion layer, fully integrated into a soft, flexible polyurethane resin layer laminated on a PET substrate containing electronic circuitry and blue LEDs. This approach can be used to integrate uniform, color-saturated, light-emitting elements in flexible electronic stacks for automotive interiors or beyond, thereby offering a viable alternative to self-emissive technologies such as OLEDs or QLEDs. Detailed measurements of the optical properties of each layer of the stack and the used QDs were incorporated into an accurate optical simulation model. Using ray tracing simulations, the thickness and QD concentration of the color converting layer were optimized to achieve the targeted color. Based on these simulation results, a 100 μm QD color conversion layer was integrated within a flexible stack consisting of a white-painted transparent lightguide, circuit-printed PET, and a highly pigmented visually shielding layer, to fabricate a demonstrator of the proposed approach. Simulations and demonstrator measurements align fairly well, with a measured on-axis luminance of 93 cd/m^2 at a luminance uniformity of 80 %. While the simulated and demonstrated efficiencies are low, the use of a more transparent light guide, QDs with higher PLQY, and/or coatings with higher reflectance, can drastically improve this efficiency. Use of printing techniques such as inkjet printing as opposed to screen printing has already demonstrated promising results in display applications [30]. Strategies such as tailoring ligand chemistry for compatibility with polymer matrices can further mitigate QD aggregation and improve photoluminescence performance [27], [31], [32]. The combination of advanced printing techniques and ligand chemistry may further improve uniformity in color and luminance output.

Typical commercial OLED displays offer color luminance values up to $1000-2000$ cd/m^2 [33]. The resulting output luminance achieved with the fabricated prototype, before placing the shielding layer, is already higher; and significant gains in efficiency could still be made. This illustrates that the presented edge-lit, QD layer based design is a viable alternative to self-emissive technologies such as OLED or QLED for thin flexible electronics integrated in soft smart surfaces.

Acknowledgment

The authors acknowledge the support of Catalisti, the Flemish Spearhead Cluster for Innovation in the Chemical and Plastics Industries.

The demonstrator was fabricated with the help of Quad Industries for the coating deposition, CMST IMEC for the LED assembly and Ascorium Industries for the final integration in a flexible polyurethane lightguide.

REFERENCES

[1] P. K. Murali, M. Kaboli, and R. Dahiya, "Intelligent in-vehicle interaction technologies," *Adv. Intell. Syst.*, vol. 4, no. 2, 2022, Art. no. 2100122.

[2] P. Godano et al., "High performance sustainable materials for automotive applications: Dream or reality," in *Proc. Veh. Tomorrow 2019*, Berlin, Germany, 2021, pp. 139–155.

[3] J. Xiao, "Haptic feedback research of human-computer interaction in human-machine shared control context of smart cars," in *Proc. 25th Int. Conf. Hum.- Comput. Interaction*, Copenhagen, Denmark, 2023, pp. 116–121.

[4] D. Blomeyer and A.-L. Schulte-Gehrmann, "Surface innovations for interiors of future vehicles," *ATZ Worldwide*, vol. 121, no. 6, pp. 48–51, 2019.

[5] Yangfeng Corporate Website, "Concept cars," 2021. [Online]. Available: https://www.yanfeng.com/en/concept-cars

[6] D. Corzo, G. Tostado-Blázquez, and D. Baran, "Flexible electronics: Status, challenges and opportunities," *Front. Electron.*, vol. 1, pp. 1–8, Sep. 2020. [Online]. Available: https://www.frontiersin.org/article/10.3389/felec.2020.594003/full

[7] Y. Wang, C. Xu, X. Yu, H. Zhang, and M. Han, "Multilayer flexible electronics: Manufacturing approaches and applications," *Mater. Today Phys.*, vol. 23, Mar. 2022, Art. no. 100647. [Online]. Available: https://linkinghub.elsevier.com/retrieve/pii/S2542529322000451

[8] I. Verboven and W. Deferme, "Printing of flexible light emitting devices: A review on different technologies and devices, printing technologies and state-of-the-art applications and future prospects," *Prog. Mater. Sci.*, vol. 118, 2021, Art. no. 100760.

[9] D. Zhang, T. Huang, and L. Duan, "Emerging self-emissive technologies for flexible displays," *Adv. Mater.*, vol. 32, no. 15, 2020, Art. no. e1902391.

[10] Q. Lin et al., "Flexible quantum dot light-emitting device for emerging multifunctional and smart applications," *Adv. Mater.*, vol. 35, no. 32, 2023, Art. no. 2210385.

[11] C. B. Murray, C. R. Kagan, and M. G. Bawendi, "Synthesis and characterization of monodisperse nanocrystals and close-packed nanocrystal assemblies," *Annu. Rev. Mater. Sci.*, vol. 30, pp. 545–610, 2000.

[12] Y. Kang et al., "Quantum dots for wide color gamut displays from photoluminescence to electroluminescence," *Nanoscale Res. Lett.*, vol. 12, no. 1, 2017, Art. no. 154.

[13] S. S. Swayamprabha et al., "Approaches for long lifetime organic light emitting diodes," *Adv. Sci.*, vol. 8, no. 1, 2021, Art. no. 2002254.

[14] Y. Huang, E. L. Hsiang, M. Y. Deng, and S. T. Wu, "Mini-LED, Micro-LED and OLED displays: Present status and future perspectives," *Light: Sci. Appl.*, vol. 9, no. 1, 2020, Art. no. 105.

[15] H. W. Chen, J. H. Lee, B. Y. Lin, S. Chen, and S. T. Wu, "Liquid crystal display and organic light-emitting diode display: Present status and future perspectives," *Light: Sci. Appl.*, vol. 7, no. 3, 2018, Art. no. 17168.

[16] Z. Luo, Y. Chen, and S.-T. Wu, "Wide color gamut LCD with a quantum dot backlight," *Opt. Exp.*, vol. 21, no. 22, 2013, Art. no. 26269.

[17] H. Fujikake and H. Sato, "Current progress and technical challenges of flexible liquid crystal displays," *Proc. SPIE*, vol. 7232, Feb. 2009, Art. no. 723202. [Online]. Available: http://proceedings.spiedigitallibrary.org/proceeding.aspx?doi=10.1117/12.808148

[18] E. Chen et al., "Flexible/curved backlight module with quantum-dots microstructure array for liquid crystal displays," *Opt. Exp.*, vol. 26, no. 3, 2018, Art. no. 3466.

[19] "Illumination design software - lighttools| synopsys," 2021. Accessed: Dec. 01, 2024. [Online]. Available: https://www.synopsys.com/optical-solutions/lighttools.html

[20] M. A. D. Maur, A. Pecchia, G. Penazzi, W. Rodrigues, and A. D. Carlo, "Efficiency drop in green InGaN/GaN light emitting diodes: The role of random alloy fluctuations," *Phys. Rev. Lett.*, vol. 116, no. 2, 2016, Art. no. 027401.

[21] W. Guo et al., "Characteristics of high power LEDs at high and low temperature," *J. Semiconductors*, vol. 32, no. 4, pp. 1–3, 2011.

[22] B. Karadza et al., "Bridging the green gap: Monochromatic INP-based quantum-dot-on-chip leds with over 50% color conversion efficiency," *Nano Lett.*, vol. 23, no. 12, pp. 5490–5496, 2023.

[23] R. L. Mays, P. Pourhossein, D. Savithri, J. Genzer, R. C. Chiechi, and M. D. Dickey, "Thiol-containing polymeric embedding materials for nanoskiving," *J. Mater. Chem. C*, vol. 1, no. 1, pp. 121–130, 2013.

[24] S. Leyre et al., "Absolute determination of photoluminescence quantum efficiency using an integrating sphere setup," *Rev. Sci. Instrum.*, vol. 85, no. 12, 2014, Art. no. 123115.

[25] B. Fraser, "Color space chromaticities and luminance," Adobe Inc., San Jose, CA, USA, Tech. Rep. Rev. 5/13/05 38, 2005.

[26] O. I. Mićić et al., "Size-dependent spectroscopy of InP quantum dots," *J. Phys. Chem. B*, vol. 101, no. 25, pp. 4904–4912, 1997.

[27] G. J. Draaisma, D. Reardon, A. P. Schenning, S. C. Meskers, and C. W. Bastiaansen, "Ligand exchange as a tool to improve quantum dot miscibility in polymer composite layers used as luminescent down-shifting layers for photovoltaic applications," *J. Mater. Chem. C*, vol. 4, no. 24, pp. 5747–5754, 2016.

[28] F. Qin et al., "Inkjet printed quantum dots color conversion layers for full-color Micro-LED displays," *Electron. Mater. Lett.*, vol. 19, no. 1, pp. 19–28, 2023.

[29] Y. Zhao, C. Riemersma, F. Pietra, R. Koole, C. D. M. Donegá, and A. Meijerink, "High-temperature luminescence quenching of colloidal quantum dots," *ACS Nano*, vol. 6, no. 10, pp. 9058–9067, 2012.

[30] Y. Duan, Y. Ye, E. Chen, S. Xu, and T. Guo, "Effect of inkjet-printed quantum dots microstructure morphology on the performance of light guide plate," *Opt. Mater.*, vol. 138, 2023, Art. no. 113654.

[31] J. Weaver, R. Zakeri, S. Aouadi, and P. Kohli, "Synthesis and characterization of quantum dot-polymer composites," *J. Mater. Chem.*, vol. 19, no. 20, pp. 3198–3206, 2009.

[32] Catalisti website, "NaPoly| Catalisti," 2025. [Online]. Available: https://www.catalisti.be/en/projects/napoly

[33] LG, "LG display LG display unveils 4th-Generation OLED panel optimized for AI era," 2025. [Online]. Available: https://www.lgcorp.com/media/release/28575#:~:text=33thantheprevious,brightnessproducedbyacandle